



HAL
open science

Influence of the charge state of 1.16 MeV/u incident ions on the desorption process

S. Della-Negra, O. Becker, R. Cotter, Y. Le Beyec, B. Monart, K. Standing,
K. Wien

► **To cite this version:**

S. Della-Negra, O. Becker, R. Cotter, Y. Le Beyec, B. Monart, et al.. Influence of the charge state of 1.16 MeV/u incident ions on the desorption process. *Journal de Physique*, 1987, 48 (2), pp.261-266. 10.1051/jphys:01987004802026100 . jpa-00210438

HAL Id: jpa-00210438

<https://hal.science/jpa-00210438>

Submitted on 4 Feb 2008

HAL is a multi-disciplinary open access archive for the deposit and dissemination of scientific research documents, whether they are published or not. The documents may come from teaching and research institutions in France or abroad, or from public or private research centers.

L'archive ouverte pluridisciplinaire **HAL**, est destinée au dépôt et à la diffusion de documents scientifiques de niveau recherche, publiés ou non, émanant des établissements d'enseignement et de recherche français ou étrangers, des laboratoires publics ou privés.

Classification
 Physics Abstracts
 79.20

Influence of the charge state of 1.16 MeV/u incident ions on the desorption process

S. Della-Negra, O. Becker (*), R. Cotter (**), Y. Le Beyec, B. Monart, K. Standing (***) and K. Wien (*)

Institut de Physique Nucléaire, B.P. N° 1, F-91406 Orsay, France

(*) Institut für Kernphysik, Darmstadt, F.R.G.

(**) John Hopkins University, School of Medicine, Baltimore, U.S.A.

(***) University of Manitoba, Winnipeg, Canada

(Reçu le 9 juin 1986, révisé le 3 octobre, accepté le 10 octobre 1986)

Résumé. — L'accélérateur linéaire d'ions lourds de l'Institut de Physique Nucléaire d'Orsay a été utilisé pour étudier l'influence de l'état de charge incident q_i des projectiles (ions Ne, Ar, Kr de 1,16 MeV/u) sur l'émission ionique secondaire à partir de films minces solides organiques et inorganiques. Le rendement d'émission ionique dépend fortement de l'état de charge q_i de l'ion incident mais aussi de la nature du projectile (numéro atomique). La variation du rendement d'émission entre les trois types de projectiles est de la forme $y \sim q_{eq}^4$, q_{eq} étant pour chaque projectile la charge d'équilibre calculée à l'intérieur du matériau.

Abstract. — The heavy ion linear accelerator of the Institut de Physique Nucléaire has been used to study the influence of the projectile charge state q_i on secondary ion emission. Ions of Ne, Ar or Kr with a velocity of 1.16 MeV/u bombarded thin films of organic and inorganic solids. The experimental arrangement is described. The ion emission yield is strongly dependent on the charge state of the incident ion q_i and of its atomic number (nature of the projectile). The emission yield between the three types of projectiles varies as q_{eq}^4 where q_{eq} is the equilibrium charge state within the material for each projectile.

When a heavy ion of several MeV/u strikes the surface and penetrates the interior of an insulating solid, a great deal of damage is created along the ion track. The incident particle loses energy predominantly through its interaction with the electrons of the solid, and much of this energy remains localized. The zone, where permanent complete damage of the surrounding bulk material is observed, has a radius of a few tens of Angstroms depending on the specific energy loss and the type of material [1, 2]. The region of small defects (« extended defects ») is however much greater with a radius of several hundred Angstroms. Effects of the bombardment are particularly noticeable on the surface, where various particles may be ejected such as for instance atoms, atomic clusters or more complex structures like very large organic molecules containing several hundred atoms [3-6].

Experimental studies of the influence of various

entrance channel parameters on the desorption process have already been carried out using beams from heavy ion accelerators [7-10]. Measurements have been made over a large mass range (N to U), as well as some measurements at high energy (up to 5 MeV/u) for projectiles of intermediate mass. These have yielded fairly complete results on the behaviour of the secondary ion yields as a function of the primary ion velocity [11]. The desorption processes depend in a complex way on the dE/dx of the ion in the material and thus on the charge of the incident ion. A variation of several orders of magnitude in yield between nitrogen and uranium has been observed in experiments at G.S.I. Darmstadt [10].

It seemed particularly interesting to exploit the properties of the Orsay heavy ion linear accelerator (the injector for ALICE) in continuing such studies. This machine can accelerate a large range of ions (from ^{12}C to ^{109}Ag or ^{134}Xe) and its energy of

1.16 MeV/u is close to the value where the desorption yield is maximum [5, 9, 11]. Experiments complementary to the previous measurements [10] have therefore been undertaken at Orsay, in collaboration with the Darmstadt group.

Here we describe the overall experimental method, and present results illustrating the influence of the incident ion charge state on the secondary ion emission from the surface. We have examined thin deposits of organic molecules as well as inorganic targets, such as thin films of CSI.

1. Experimental method.

1.1 GENERAL DESCRIPTION. — The ion beam from the linear accelerator is focused onto an area of several mm² on a very thin carbon foil ($\sim 20 \mu\text{g}/\text{cm}^2$) at the centre of a reaction chamber. In passing through the foil the ions lose a certain number of electrons and emerge with a distribution of charge states. Figure 1 shows the distributions measured by E. Baron [12] for the ions used here (Ne, Ar and Kr).

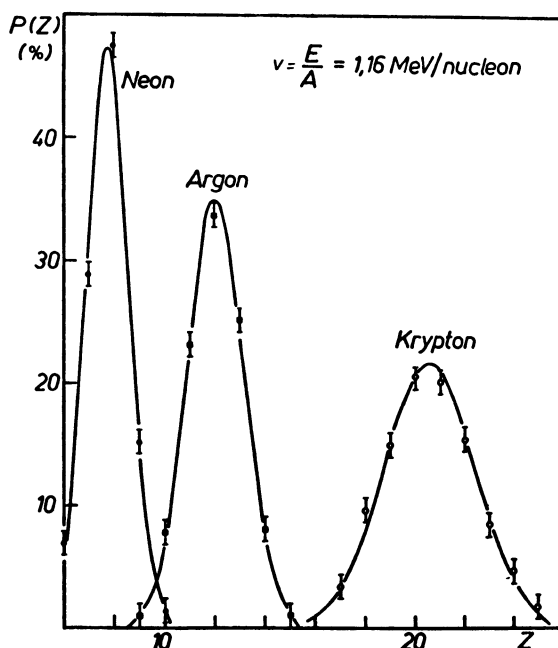


Fig. 1. — Charge distribution after passing through a $20 \mu\text{g}/\text{cm}^2$ carbon foil and measured after the magnetic analyser (from Ref. [12]).

At 50 cm from the centre of the chamber there is a slit of variable width (2 to 10 mm). It is mounted on a sliding window which serves as the entrance port of a movable magnet (radius = 0.8 m, $B_{\text{max}} = 1.5$ tesla).

The angle of this magnet entrance slit with respect to the centre of the chamber can be set very precisely, so it is possible to accept the beam elastically scattered through a well-defined angle. The beam intensity is controlled by varying the angle (usually $< 5^\circ$).

The different charge states of the scattered ion beam can be separated by varying the magnetic field. Measurement of the magnetic field strength determines the charge state selected.

The energy of the beam scattered through a given angle can be calculated classically (elastic scattering) and for the small angles used (a few degrees) the energy of the scattered ions is close to the incident energy. Likewise the energy loss in the carbon foil is small (~ 1 MeV for ^{84}Kr).

Figure 2 shows a schematic diagram of the experimental arrangement (magnet + spectrometer). At the exit of the magnet there is a device for measuring and viewing the beam, then the time-of-flight spectrometer. Figure 3 shows a schematic diagram of the spectrometer, which has already been described in reference [9]. Detector D1, which usually measures the time of arrival of the primary ions in order to determine their velocity, is used here to control and adjust the scattered beam intensity before starting an experiment. During measurements this detector is swung out of the beam to the position shown.

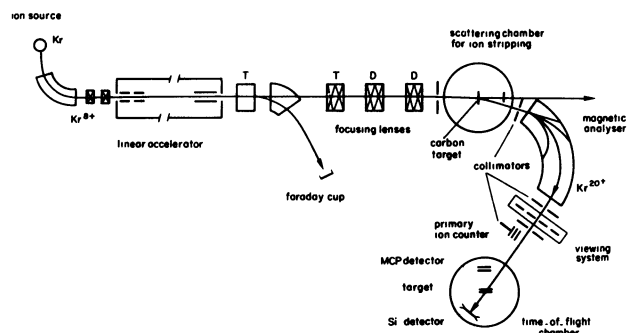


Fig. 2. — General view of the experimental equipment.

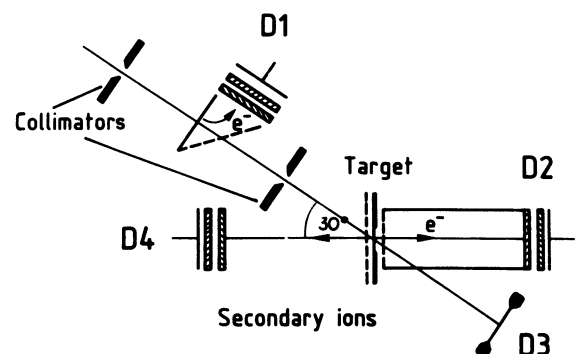


Fig. 3. — Schematic diagram of the apparatus for measuring secondary ions and electrons.

Secondary ions ejected from the target are accelerated by a fine grid at a potential of 6 kV, then recorded by detector D4, a pair of microchannel plates. This provides the « stop » signal for measuring their time-of-flight.

Detector D3 is a 150 μm Si detector which is used to monitor the incident beam after it passes through the target. The signal corresponding to the arrival of each primary ion at the Si detector provides the « start » signal for measuring the time-of-flight of the secondary ions. Detector D3 also measures the primary ion energy, so it is possible to set a coincidence window in the energy spectrum. Secondary ions are thus recorded only when the corresponding primary ion has the correct energy. This is particularly important when the selected ion beam is rather impure, as shown in figure 4. It was found possible to reduce the parasitic peaks greatly by adjusting the operating parameters of the accelerator, but in any case the coincidence window selected only those events produced by primaries of the correct energy.

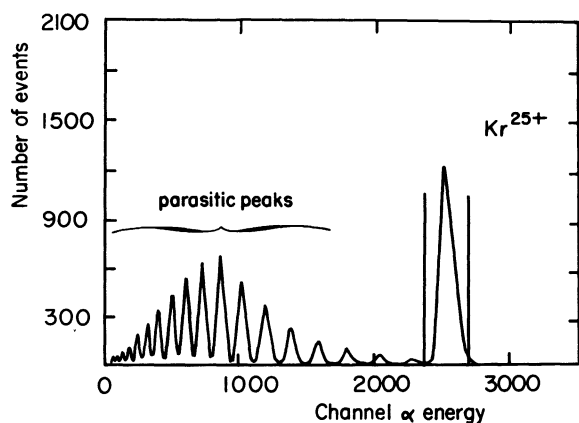


Fig. 4. — Ion energy spectrum measured with a silicon detector. The peak corresponding to Kr^{25+} is indicated in the figure together with the limits of the coincidence window.

The following table shows the ions and the selected charge states for the first experiments carried out with this experimental arrangement.

Projectile	Accelerated charge state	Range of charge states used
—	—	—
Ne	2^+	$4^+ \text{ à } 10^+$
Ar	4^+	$7^+ \text{ à } 15^+$
Kr	7^+	$12^+ \text{ à } 25^+$

Thin deposits of caesium iodide and phenylalanine ($\text{C}_9\text{H}_{11}\text{O}_2\text{N}$) were prepared by vacuum evaporation onto aluminized mylar. The thickness of the deposits was $\sim 2000 \text{ \AA}$ so as to obtain a homogeneous target. The ions emitted by bombardment with primary ions of several MeV/u are well known and exhibit characteristic peaks in the time-of-flight spectrum [9, 10]. Positive or negative ions are detected when the acceleration grid is at a negative or positive potential respectively. Figure 5 shows an example of a time of flight spectrum obtained from the phenylalanine target. The molecular

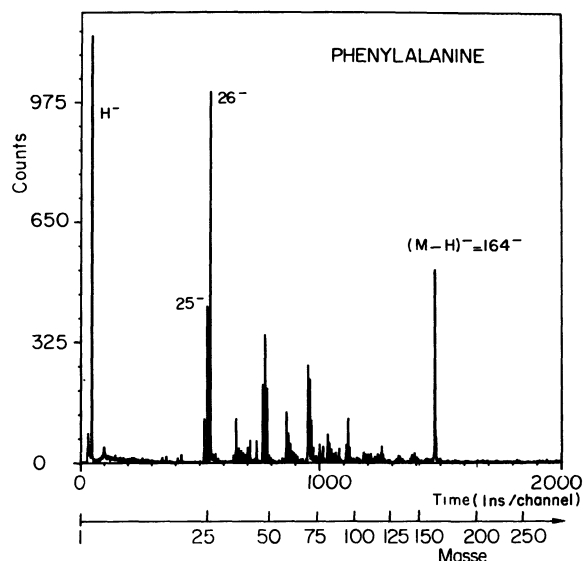


Fig. 5. — Example of a time of flight mass spectrum for an organic solid — phenylalanine — the molecular ion $(\text{M} - \text{H})^-$ is clearly visible. This spectrum is obtained from only about 5 000 Kr ions incident on the target.

ion $(\text{M} - \text{H})^-$ at mass 164 u is one of the dominant peaks.

1.2 MEASUREMENTS OF SECONDARY ION YIELDS. —

The collimators shown in figure 3 were carefully aligned to ensure that every primary ion passing through the target struck the Si detector. The number of primary ions with a selected charge state was obtained by integrating the selected peak in the energy spectrum of this detector. The number of secondary ions of mass M was obtained by integration of the corresponding peak in the time-of-flight spectrum, coincident with events in the primary energy window. The yield is the ratio of the number of secondary ions to the number of primary ions.

The primary ion beam is pulsed, with a repetition frequency of 24 MHz. In order to avoid a second primary ion striking the target after the start of a time interval triggered by a given primary ion, it was necessary to limit the number of primary ions to 1 000 per second or less.

The time-of-flight measurements of the secondary ions were carried out with a time digitizer (TDC) which can accept 255 stop signals for each start [13]. However, if several ions of the same mass are ejected by a given primary ion, their times of flight are the same, and the TDC delivers only a single output. The measured yields have been corrected for this effect by assuming a Poisson distribution for the emitted ions. The following relation then gives the total yield Y_t for an ion of given mass, corresponding to a measured yield Y_m [7]:

$$Y_t = \left(-\frac{1}{p}\right) \ln(1 - Y_m).$$

Here p is the overall detection efficiency for ions of the given mass. For measurements of the relative yields as a function of the incident ion charge state, it is necessary only that p is independent of this parameter. For a measured yield $y_m = 0.3$, for instance, the total yield y_t reaches 0.36, or for $y_m = 0.9$ it is 2.3.

2. Experimental results and discussion.

During all the experiments the targets were kept in place in the spectrometer and a pressure of 10^{-6} torr was maintained with a turbomolecular pump.

2.1 CAESIUM IODIDE TARGET. — The variation of the emission yield of the secondary ions Cs^+ and $(\text{CsI})\text{Cs}^+$ as a function of the primary charge state is shown in figure 6 for the three types of primary ions used, neon, argon and krypton. Since H^+ ions are always desorbed abundantly, their emission yield is also given in the figure. The yields for different incident ions are directly comparable.

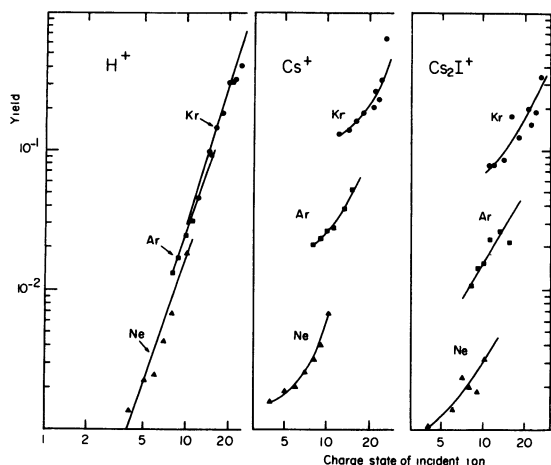


Fig. 6. — Variation of desorption yield as a function of the charge state for the ions H^+ , Cs^+ , $(\text{CsI})\text{Cs}^+$ from a caesium iodide target. All yields may be compared directly but the yields per incident particle are only relative. The lines serve as guide to the eyes.

Figure 7 shows similar results for negative secondary ions, including the ion of mass 24 (C_2^-), which is always present in the negative spectrum. We note that the q_i dependence for C_2^- is very different from the q_i dependence for the ions characteristic of the thin film itself.

The results shown in figures 6 and 7 for bombardment of a CsI target by primary ions of well defined charge q_i show clearly the importance of this parameter in the desorption process.

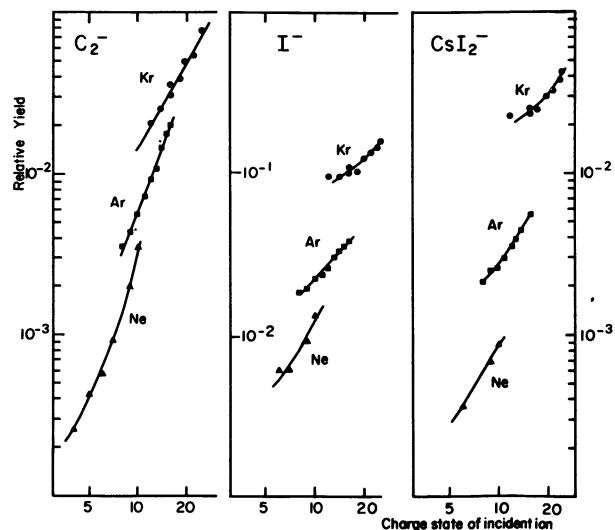


Fig. 7. — Variation of desorption yield as a function of the charge state for the ions C_2^- , I^- and $(\text{CsI})\text{I}^-$ from a caesium iodide target. See caption to figure 6.

2.2 PHENYLALANINE TARGET. — This molecule was chosen since it had already been used in experiments studying the effect of incident ion velocity on desorption [10]. Moreover, thin films of this compound can be prepared without altering its structure, in contrast to most other organic molecules.

Figure 8 shows the variation of emission yield for the negative molecular ion $(\text{M}-\text{H})^-$ as well as for the ions H^- and 26^- (C_2H_2^- or CN^-). Figure 9 shows similar results for the positive ions H^+ , C^+ and NH_4^+ ejected from the same target. Yields for the positive molecular ion $(\text{M}+\text{H})^+$ and for $(\text{M}-\text{C}_2\text{OH})^+$

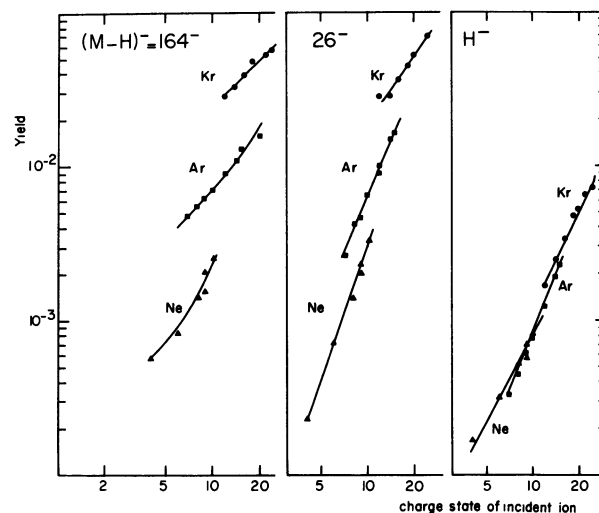


Fig. 8. — Variation of desorption yield as a function of the charge state for the ions $(\text{M}-\text{H})^-$, C_2H_2^- or $(\text{CN})^-$ and H^- from a phenylalanine target. See caption to figure 6.

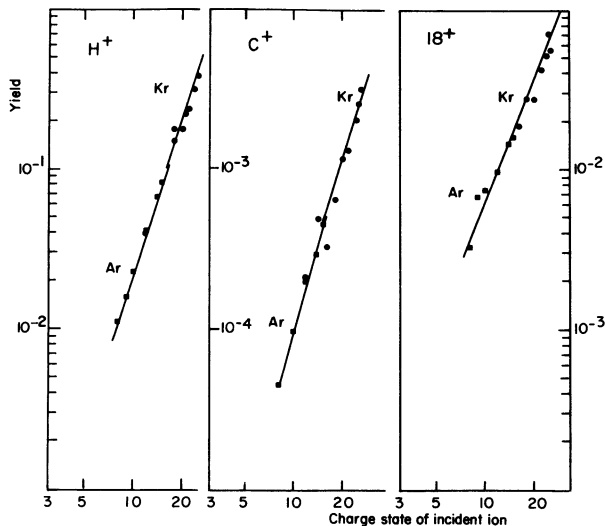


Fig. 9. — Variation of desorption yield as a function of the charge state for the ions H^+ , C^+ and NH_4^+ from a film of phenylalanine. See caption to figure 6.

were measured recently using a different phenylalanine target. For all these ions (and also Cs^+ ...) there is a q_i dependence which is different with Ne, Ar and Kr projectiles. Our results agree with those obtained earlier by other authors [14-16] for low charge states ($q_i < 13$) and relatively light projectiles. Here the q_i dependence extends to larger q_i values and heavier projectiles. The comparison of the yield curves between the three different projectiles shows a larger variation of slope for low charge states than for high ones. Also, at the same incident charge state, the yields increase with the atomic number of the projectile.

However certain ions like H^+ , C^+ , NH_4^+ (a fragment from the phenylalanine molecule) behave differently and have yields $\gamma \alpha q_i^n$ with $n \sim 4$ whatever the incident ion. A similar observation was made in the experiments at GSI Darmstadt [17]. It probably indicates that these ions originate close to the point of impact of the primary ion, where the radiation damage is large. On the other hand, the atomic ions I^- or Cs^+ , and the organic molecular ions may come also from regions far from the point of impact. The relation between the energy deposited in the medium and the emission from the surface is then less direct, but the effect of the incident ion charge is still clearly present.

2.3 CHARGE STATES OF THE PRIMARY ION. — The average charge states of heavy ions after passing through thin carbon foils can be predicted fairly well with the use of semi-empirical formulas [12, 18-20]. The charge distributions, on the other hand, are more difficult to predict since they can depend on the atomic shell structure of the projectile [20].

Although such distributions can be measured easily

after the ion has passed through the foil, they give little information on the distribution function in the interior of the material, which is still poorly known. Indeed, according to Betz and Grodzins [22], the charge state of an ion increases rapidly while leaving the material, since the excitation of the projectile leads to the ejection of several Auger electrons. In this picture, the mean charge and the experimental charge distribution are the results of charge exchanges in the interior of the material followed by de-excitation outside. There will therefore be only a relatively small variation of the charge inside the material.

On the other hand, the theory of Bohr and Lindhart [23] assumes a variation of the charge state in the material as a result of successive collisions between the projectile and the electrons of the target material. An average equilibrium charge $\langle q_{eq} \rangle$ is expected to be reached after a certain distance of penetration. Bohr [24] has suggested a relation between the charge $q(x)$ and the thickness traversed x :

$$q(x) = q_{eq} + (q_i - q_{eq}) e^{-Kx}.$$

q_{eq} is the final equilibrium charge for the ion considered, q_i its initial charge, and K is a parameter which depends on the projectile and the target material, and which can be determined experimentally. However, experimental values of K refer always to the change after passing through a thickness x of material.

The evolution of the charge state inside the material is at present the object of theoretical calculations [25], which should soon be applicable to the case of desorption in simple materials.

In fact, the influence of the charge state of the ion as it passes through the material is also felt on the surface and the total yield depends in a complex way on the energy loss $dE(x)/dx$ and therefore on $q(x)$ as a function of the distance x of penetration. As Nieschler *et al.* have already pointed out [14], the initial charge state acts only as a fixed parameter, and the experimental values of desorption yields depend also on the cumulative effect of the charge exchange processes in the interior of the medium. The real dependence on the incident charge state q_i is therefore hidden. For light ion projectiles, Nieschler *et al.* concluded from their measurements that the depth of penetration below which the effect at the surface was no longer apparent was smaller than the depth required to attain charge equilibrium. According to our preliminary comparisons with theory for primary ions of high charge state, the conclusions of Nieschler *et al.* are mainly valid for light ions, for which the energy losses dE/dx are smaller and for which the variation of the charge state as a function of the thickness traversed is more rapid.

The equilibrium values of the charge state in the CsI and phenylalanine targets can be estimated according to Shima *et al.* [21] for incident ions of Ne, Ar or Kr. They are (6.85), (11.06) and (19.06), respectively. For

these three incident ions, the variation of desorption yield Y (at 1.16 MeV/u) for $q = q_{eq}$ deduced from the experimental curves of figures 6, 7 and 9 is given by a relation of the form $y \propto q_{eq}^4$ when the yield is treated as a function of the equilibrium charge of each incident projectile.

3. Conclusion.

We have presented new experimental results on the secondary ion emission from surfaces under the impact of ~ 1 MeV/u ions. It has been shown that the variation of the desorption yield with the incident charge state depends also on the type of projectiles. Charge changing in a medium as a function of the depth of penetration varies from one projectile to another one [25] and the knowledge of the variation of the charge inside the material is certainly needed to explain the different shapes of the yield curves. Calculation using the results of these authors [25] will be published shortly. The ions, neutral atoms, and electrons emitted

from the surface are observables which give information about the internal perturbations produced in the material by the incident ions of the beam. It should also be possible to measure in the near future the charge states of ions leaving the surface of the material, since the desorption yield is very sensitive to the charge state.

The experimental set up together with the data acquisition system for this type of experiment constitutes a unique facility for the present study of the interactions between MeV ions and materials, particularly material surfaces.

Apart from the fundamental aspects it is clear that an analytic program using highly charged ions of energy ~ 1 MeV/u is a particularly useful probe for identification of molecules deposited on a surface.

Acknowledgment.

We are very grateful for the efficient assistance provided by the technical staff of the linear accelerator (G. Coeur Joly, J. C. Dubois, P. Nael, J. C. Potier).

References

- [1] DARTYGE, E., DURAUD, J. P., LANGEVIN, Y. and MAURETTE, M., *Phys. Rev. B* **23** (1981) 5213.
- [2] ALBRECHT, P., AMSBRUSTER, P., SPOHR, R., ROTH, M., SCHAMPERT, K. and STARHRMANN, H., *Appl. Phys. A* **37** (1985) 37.
- [3] Nordic Symposium on « ion deduced desorption of molecules from bio-organic solids », *Nucl. Instrum. Meth.* **198** (1982) 1-169.
- [4] Texas Symposium on particle induced desorption mass spectrometry, *Int. J. Mass. Spectros. Ion Phys.* **53** (1983) 1-362.
- [5] DELLA-NEGRA, S. and LE BEYEC, Y., *Nucl. Sci. Appl.* **1** (1983) 569.
- [6] SUNDQVIST, B. and MACFARLANE, R., *Mass Spectr. Rev.* **4** (1985) 421.
- [7] HAKANSSON, P., KAMENSKY, I. and SUNDQVIST, B., *Nucl. Instr. Meth.* **198** (1982) 43 ;
HAKANSSON, P. and SUNDQVIST, B., *Rad. Effect* **61** (1982) 179.
- [8] VOIT, H., NEES, B., NIESCHLER, E. and FRÖLICH, H., *Int. J. Mass. Spectros. Ion Phys.* **53** (1983) 201.
- [9] DELLA-NEGRA, S., JACQUET, D., LORTHOIS, I., LE BEYEC, Y., BECKER, O., WIEN, K., *Int. J. Mass. Spectros. Ion Phys.* **53** (1983) 215.
- [10] GUTHIER, W., BECKER, O., DELLA-NEGRA, S., KNIPPELBERG, W., LE BEYEC, Y., WEIKERT, U., WIEN, K., WIESEN, P. and WURSTER, R., *Int. J. Mass. Spectros. Ion Phys.* **53** (1983) 185.
- [11] BECKER, O., DELLA-NEGRA, S., LE BEYEC, Y. and WIEN, K., *Nucl. Instrum. Meth. and Phys. Res.* **B 16** (1986) 321.
- [12] BARON, E., Thesis, Université Paris-Sud Orsay (1975).
- [13] FESTA, E., TASSON-GOT, L., SELLEM, R., *Nucl. Instrum. Meth. A* **234** (1985) 305.
- [14] NIESCHLER, E., NEES, B., BISHOP, N., FRÖLICH, H., TIERETH, W. and VOIT, H., *Rad. Effect* **83** (1984) 121.
- [15] HAKANSSON, P., YAYASINGHE, J., JOHANSSON, A., KAMENSKY, I. and SUNDQVIST, B., *Phys. Rev. Lett.* **47** (1981) 1227.
- [16] MEINS, C. K., GRIFFITH, J. E., QIER, Y., MENDENHALL, M. H., SEIBERLING, L. E. and TOMBRELLO, T. A., *Rad. Eff.* **71** (1983) 13.
- [17] WIEN, K., BECKER, O., GUTHIER, W., to be published in *Nucl. Instrum. Meth.*
BECKER, O., GUTHIER, W., WIEN, K., DELLA-NEGRA, S., LE BEYEC, Y. and COTTER, R., *Ion Formation from Organic Solids*, Springer Series in Chemical Physics, ed. A. Benninghoven, 1986, p. 11.
- [18] BAUDINET-ROBINET, Y., *Nucl. Instrum. Meth.* **190** (1981) 197.
- [19] KNYTAUSTAS, E. J. and JOMPHE, M., *Nucl. Instrum. Meth.* **23** (1981) 679.
- [20] SHIMA, K., ISHIHARA, T., MIYASHI, T., MIKUMMO, T., *Phys. Rev. A* **28** (1983) 2162.
- [21] SHIMA, K., ISHIHARA, T., MIKUMMO, T., *Nucl. Instrum. Meth.* **200** (1982) 605.
- [22] BETZ, H. D. and GRODZINS, L., *Phys. Rev. Lett.* **25**, 4 (1970) 211.
- [23] BOHR, N. and LINDHARD, J., *Dan. Vid. Selsk. Mat. Fys. Medd* **25**, n° 13 (1964).
- [24] BOHR, N., *Phys. Rev.* **59** (1941) 270.
- [25] MAYNARD, G. and DEUTSCH, C., to be published ; and the proceedings of the 1st Workshop on « Physics of Small Systems » (1986). *Lecture Notes in Physics*. Eds. E. Hilf and K. Wien (Springer Series), in press.